ISSN 0001-4338, Izvestiya, Atmospheric and Oceanic Physics, 2008, Vol. 44, No. 4, pp. 448–458. © Pleiades Publishing, Ltd., 2007.
Original Russian Text © A.V. Polyakov, Yu.M. Timofeev, Ya.A. Virolainen, 2008, published in Izvestiya AN. Fizika Atmosfery i Okeana, 2008, Vol. 44, No. 4, pp. 483–493.

Polar Stratospheric Clouds from Satellite Observational Data

A. V. Polyakov, Yu. M. Timofeev, and Ya. A. Virolainen

Research Institute of Physics, St. Petersburg State University, Ul'yanovskaya ul. 1, Petrodvorets, 198904 Russia
e-mail: tim@troll.phys.spbu.ru

Received October 3, 2007

Abstract—The spectral aerosol-attenuation coefficients (SAACs) obtained from SAGE III measurements are used to study the physical and integral microphysical characteristics of polar stratospheric clouds (PSCs). Different criteria for PSC identification from SAAC measurements are considered and analyzed based on model and field measurements. An intercomparison of them is performed, and the agreement and difference of the results obtained with the use of different criteria are shown. A new criterion is proposed for PSC identification, which is based on the estimate of how close the measured vector of the spectral attenuation coefficient is to a model distribution of the PSC ensemble. On the basis of different criteria, cases of PSCs are isolated from all SAGE III observations (over 30000). All selection criteria lead to a qualitatively and quantitatively similar space–time distribution of the regions of PSC localization. The PSCs observed in the region accessible to SAGE III measurements are localized in the latitudinal zones 65°–80° in the Northern Hemisphere and 45°–60° in the Southern Hemisphere during the winter–spring period. In the Northern Hemisphere, PSCs are observed within the longitudinal zone 120° W–100° E with the maximum frequency of PSC observation in the vicinity of the Greenwich meridian. In the Southern Hemisphere, the region of PSC observation is almost the same in longitude but with a certain shift in the maximum frequency of PSC observation to the west. This maximum is observed in the vicinity of 40°W, and the region of usual PSC observation is the neighborhood of 60° of the maximum's longitude. The physical parameters of PSCs are estimated: the mean heights of the lower and upper boundaries of PSCs are 19.5 and 21.9 km, respectively, and the mean cloud temperature is 191.8 K. The integral microphysical parameters of PSCs are estimated: the total surface of NAT particles $S_{NAT} = 0.41$ $\mu m^2/cm^3$; the total volume of NAT particles $V_{NAT} = 1.1$ $\mu m^3/cm^3$; and, for all aerosol and cloud particles together, S is 2.9 ± 1.5 at a standard deviation of 2.7 $\mu m^2/cm^3$ and V is 2.8 ± 1.5 at a standard deviation of 4.2 $\mu m^3/cm^3$. A high frequency of PSC occurrence and high values of S and V in PSCs both for all particles and for NAT particles have been noted in January–February 2005 as compared to the rest of the period of SAGE III measurements for 2002–2005.

DOI: 10.1134/S0001433808040051

INTRODUCTION

Polar stratospheric clouds (PSCs) are of considerable importance in the chemistry of ozone, because heterogeneous reactions, which affect the gas composition of the atmosphere, in particular, the content of chlorine and nitric compounds actively participating in the destruction of ozone, occur on their surfaces [1, 2]. PSCs are also important for the radiation balance of the stratosphere and can result in significant variations in air temperature in the polar regions in winter [3]. In this connection, studies of the chemical, microphysical, and optical characteristics of PSCs are of great interest.

PSCs form at heights of 15 to 30 km at extremely low temperatures (observed under conditions of polar winters in the stratosphere of both hemispheres) during joint condensation of water vapor and nitric acid on sulfate particles of the background stratospheric aerosol (BSA) and, in some cases, as particles freeze [4]. These clouds differ in chemical composition and microphysics. In fact, the term PSCs combines different types of stratospheric clouds, which is reflected in a special classification of PSCs [5]. PSCs of type II are observed at temperatures below the freezing point of ice (of about 188 K) and consist of water ice. PSCs of type I (clouds that consist of a solution of nitric acid and water) are observed at higher temperatures; in this case, PSCs of type Ib consist of small particles in the form of a supercooled three-component solution ($H_2SO_4/HNO_3/H_2O$), whereas clouds of type Ia consist of larger crystalline hydrates of nitric acid (nitric acid trihydrate (NAT) or nitric acid dihydrate (NAD)). A detailed numerical simulation of PSCs was performed in a number of studies (see, for example, [6, 7]). On the basis of such a simulation, the statistical characteristics of the microphysical and optical parameters of PSCs were studied [8, 9].

The study of PSCs started in 1978–1979 with the first satellite observations in the polar regions with the aid of the instruments of SAM II [10]. Later, PSCs were studied by taking satellite measurements with different satellite instruments (SAGE I, SAGE II, POAM II, POAM III, CLAES, ILAS II, MIPAS), ground-based lidar measurements, and different direct

and indirect measurements of the optical and microphysical characteristics of PSCs in special aircraft and balloon experiments (see, for example, [11]).

Satellite measurements of spectral aerosol attenuation coefficients (SAACs) (primarily with the aid of the occultation method) made it possible to study the frequency (probability) of occurrence of PSCs, their seasonal cycle, location (latitudinal and longitudinal variations), heights, and the relation between PSC characteristics and atmospheric temperature and dynamics (for example, [4, 10, 12–14]). SAAC satellite measurements in the visible and IR regions of the spectrum were also used to determine the chemical composition of PSCs and a number of their microphysical characteristics. For example, in [15], the results of ILAS II measurements in the IR region (June–August 2003) were used to determine the composition of PSCs and the effective radius of their particles. A method of determining the volumes and areas of particles using data from different satellite instruments (SAM II, SAGE II, POAM II) is proposed in [16]. The results of dividing clouds into two types—Ia and Ib—according to satellite observations are given in [5]. The spectral IR measurements of atmospheric self-radiation with the MIPAS instrument were used in [17] to study the evolution of PSCs in winter.

This paper is devoted to analysis of the characteristics of PSCs using SAGE III data obtained in 2002–2005. Earlier, the data obtained with this instrument were used to study the ozone content and integral microphysical characteristics of BSA [18–20].

2. CRITERIA OF PSC IDENTIFICATION

When different characteristics of PSCs are studied, the criteria of their identification in satellite data are very important. First, only one criterion was used—the SAAC value near the wavelength of 1 μm (the SAM II instrument had only one measuring channel). The occurrence of PSCs was associated with an excess SAAC value for the stratosphere near 1 μm over 0.0008 km^{-1} [10]. This criterion made it possible to identify any stratospheric clouds. Later, particularly in connection with the advent of multichannel spectral instruments, more complex criteria were used: from (i) comparison of the SAAC with the Rayleigh attenuation coefficient [12], (ii) the vertical dependence of the SAAC, (iii) the ratio of SAAC values at different wavelengths (for example, at 525 and 1000 nm [21, 22]), (iv) comparison of the SAAC with its mean background values, (v) the height at which measurements are interrupted because of high absorption, (vi) atmospheric temperature, etc. [13, 23, 24]. In [25], an algorithm for identifying PSCs is proposed for the SAGE III multichannel instrument, which is based on SAAC measurements at three wavelengths: 525, 1020, and 1550 nm. A variety of chemical, microphysical, and optical characteristics of PSCs makes the problem of identifying PSCs from SAAC measurements alone difficult and gives ambiguous results (see, for example, [26]).

In order to analyze the criteria of identifying PSCs from the SAAC measurements, we used two model statistical ensembles of stratospheric states. The first is a combined microphysical and optical model of the BSA and is described in [27]. The other is constructed on the basis of a microphysical model of PSCs [6, 7], which is supplemented with the PSC optical characteristics calculated in [8, 9]. The latter model of PSCs was developed to simulate the formation, increase, and evaporation of particles along air trajectories in the Arctic stratosphere. A large number of long-term trajectories from the data of the United Kingdom Meteorological Office (UKMO) that make it possible to construct a three-dimensional pattern of the evolution of the arctic vortex, were calculated for the Arctic winter of 1999–2000. The simulation covered the period of November 1, 1999–April 15, 2000. Several scenarios were used to construct PSC ensembles. These scenarios differed in a number of assumptions on the microphysical parameters and processes that control PSC formation and transformation. The results of the simulation of PSCs were carefully compared to the data obtained during the SOLVE measuring campaign [7] and earlier experiments [28, 29]. In order to describe the microphysical properties and the corresponding optical characteristics, we considered the total ensemble of PSCs, which included realizations of stratospheric aerosol from the four models (Het0many.sed, Het16many.sed, Met_1_m10.once.sed, and Nadhet1many.sed) that agreed best with experimental data. The total ensemble of stratospheric aerosol and PSCs consisted of 255 949 realizations. Note that the maximum of the size distribution function (SDF) of BSA particles (liquid and SAT) corresponds to sizes on the order of tenths of a micron, while the maximum of PSC particles (NAT and water ice) corresponds to sizes on the order of microns. It is this difference in the mean sizes of particles that leads to a different spectral behavior of the SAAC for the BSA and PSCs, and it is used in several of the aforementioned methods.

In addition to the three earlier proposed criteria of identifying PSCs (see Table 1), we use a new method. Since we have statistical models (samples, ensembles) of atmospheric states that correspond to the BSA [27] and PSCs [8, 9], we use our own criterion of identifying PSCs, which is based on more modern approaches and on the use of the statistics of the clouds under study rather than of arbitrary clouds. The calculations of the mean SAACs, spectral covariance matrices, and their eigenvectors and eigenvalues for the BSA and PSCs have shown that the mean spectral behaviors of these characteristics are less pronounced for PSCs than for the BSA, a result that points to a larger contribution to the SAAC from large particles in PSCs as compared to the BSA.

Table 1. Criteria of cloud identification (the condition of cloud observation is formulated)

Arbitrary name	Notation	Criteria	Ссылка
Attenuation at 1 μm	1	SAAC at 1 μm is larger than 0.0008 km^{-1}	[10]
Two points of the spectrum	2	SAAC at the wavelength 0.52 μm is less than two times greater than that at 1 μm	[22]
Three points of the spectrum	3	Plane points whose coordinates are equal to the SAAC ratio for wavelength pairs lie within a given rectangle	[25]
Closeness to the linear subspace of PSCs	V_3	SAAC vector is closer to the n-dimensional subspace of PSCs than to the subspace of the BSA	This paper

Table 2. Number (percentage) of correct identifications of PSCs and the BSA

Criterion	% of correct identifications	
	in aerosol sampling	in PSC sampling
1	87	39
2	94	59
3	96	43
V_3	99.8	63.9

Table 3. Number of PSC observations selected from real data

	1	2	3	V_3
1	149	122	108	118
2	122	222	152	161
3	108	152	152	126
V_3	118	161	126	343

Our estimates show that, at a real error of SAAC measurements (from 3–10 to 100% for the SAGE III data; see details in Section 3.4), two eigenvectors of the SAAC covariance matrix are sufficient for an optimal approximation of nearly any realization. In this case, calculations have shown that the first three vectors of the SAAC covariance matrices for the PSC and BSA ensembles noticeably differ in pairs, which has made it possible to use optimal expansions in terms of the proper basis to identify PSCs. Therefore, the proposed method is based on the criterion of the best approximation of measured PSCs by the proper orthogonal basis v_n. This implies that, if the first n vectors of the PSC ensemble approximate the vector of observed SAACs more closely than the n vectors of the BSA ensemble, then PSCs are observed. Since the numerical model of [6, 7] reproduces not only PSCs but all states of stratospheric aerosol, in constructing this criterion, as a PSC ensemble we used a narrower ensemble for which only the PSC realizations were selected. To this end, we used the criterion that characterizes the SAAC at a wavelength of 1.020 μm [10] and eliminated the realizations in which the SAAC is less than 0.0008 km^{-1}. As a result, 100 514 realizations remained. Although, in general, the criterion of [10] identifies any clouds, in this case, the initial ensemble did not include clouds differing from PSCs; therefore, the resulting subensemble also contains just PSCs. The estimates have shown that the optimal number of the expansion vectors is 3; below, we denote this criterion V_3.

The verified criteria of identifying PSCs are summed based on the ensemble of model stratospheric states in Table 1. Numerical analysis using model and real data has shown that different criteria yield different PSC ensembles. Table 2 shows the percentage of cases of successful identification of PSCs and the BSA with model data [7, 27]. Note that the percentage of cases of PSC identification in "PSC sampling" is far from 100, because this sampling includes all stages of PSC development and degradation, including the states (indistinguishable from the background aerosol) at the times of cloud origination and collapse. It follows from Table 2 that the V_3 criterion makes it possible to correctly classify observations in most of cases, which suggests its advantage over other criteria. The data in Table 2 also show noticeable mutual differences in the results of identification of PSCs when different methods are used.

This is also supported by Table 3, which gives the results from different methods of analyzing the real SAGE III data on SAACs. As an example, Table 3 gives the number of PSCs identified in the SAGE III measurements over the entire observation period (2002–2005) according to different criteria and the frequency of overlapping, i.e., the number of PSCs identified simultaneously by two methods (nondiagonal elements in the table). It follows from the given data that the criteria being used can noticeably affect the number of identified PSCs, thus affecting the estimates of different climatological characteristics of PSCs. However, it is interesting that many of the results obtained for different criteria (see the next section) were close to one another, so that it is possible to suggest an objective character of the criteria. It should also be noted that, in order to exclude other types of cloudiness in further analysis, the following two limitations were additionally used: (1) the air temperature at an observed height must not exceed 196 K and (2)

the height of observations must be within a range of 15–30 km.

3. RESULTS

3.1. Features of Observations

Before analyzing the results, it is necessary to note the specific character of the spatiotemporal distribution of the SAGE III data, caused by the use of the occultation method and the parameters of the satellite's orbit [20]. Table 4 gives the periods of the year and zones in the mid- and polar latitudes in which the measurements under consideration were performed.

It follows from Table 4 that the measurement latitude varies very slowly with time; the measurement latitude changes one degree (111 km) over the course of 5–10 or more days. At the same time, over 24 h, the instrument takes 26 measurements with a uniform step in longitude (equally for the Northern and Southern hemispheres). As a result, the measurement data are inconvenient for study latitudinal variations in atmospheric parameters and are of limited interest in studying their variability; however, these data are informative with respect to the longitudinal distributions of the observed parameters.

Let us note the facts that are important for analyzing PSC observations. The observations were active within the latitudes characteristic of PSCs for limited time periods: north of 65° N (September–March) and south of 50° S (April–September). In this case, the observation latitude does not exceed 80° N in the Northern Hemisphere and does not extend south of 58° S.

3.2. Spatial Distribution of PSCs

Figure 1 gives the number of PSC observations in accordance with different criteria within a longitudinal interval 10° wide. It shows the following.

(1) All selection criteria result in a qualitatively and quantitatively similar spatial arrangement of the regions in which PSCs are localized.

(2) The PSCs observed in the region accessible to the SAGE III measurements are localized in the latitudinal zones 65°–80° in the Northern Hemisphere and 45°–60° in the Southern Hemisphere.

(3) In the Northern Hemisphere, PSCs are observed within the longitudinal zone 120° W–100° E, with the maximum frequency of PSC observation near the Greenwich meridian. In the Southern Hemisphere, the longitudinal distribution of PSCs has a similar form, but with a certain westward shift in the maximum frequency of PSC observation. Here, PSCs are usually observed in a 120° longitudinal sector with the center at 40° W.

Table 4. Periods and latitudinal zones within which the SAGE III measurements were performed

Northern Hemisphere		Southern Hemisphere	
Period	Latitudinal zone	Period	Latitudinal zone
March–June	77–48	January–May	35–58
July–September	48–80	May–January	58–36
October–December	80–65		
January–February	65–77		

3.3. Time Distribution of PSCs

Recall that the discovered properties of the time distribution of PSCs can also be related to the properties of both the orbit and the relation between the time and latitude of the SAGE III measurements (see Table 4). Figure 2 shows the seasonal distribution of PSC occurrence in the SAGE III observations (averaging over four years of observations). Analysis of Fig. 2 primarily shows that all criteria of PSC identification yield a qualitatively similar pattern of the seasonal distribution of the number of PSC observations. One can note the basic regularity with which PSCs are observed in winter in both the Northern (November–February) and Southern (May–September) hemispheres. The absence of PSCs in spring is explained by a decrease in the latitude of observations in March for the Northern Hemisphere and in October for the Southern Hemisphere (see above).

3.4. Determination of the Integral Aerosol Microphysical Parameters of the Stratosphere

Our investigations [8, 9] have shown that the information contained in the SAAC data obtained from SAGE III measurements makes it possible to estimate the total area S and total volume V of aerosol-cloud particles (there are difficulties in direct separation based on optical measurements of the particles of stratospheric aerosol and PSCs). Moreover, statistical estimates have indicated that it is also possible to retrieve the area S_{NAT} and volume V_{NAT} of NAT particles (crystalline hydrate of nitric acid) owing to a distinct difference in size between these particles and the particles of sulfuric acid aerosol.

Using the data of calculations [6–9] and the same criteria of PSC identification (Table 1), we have constructed the corresponding solution operators via linear regression. In this case, the solution can be written as

$$x = \bar{x} + K_{xy}(K_{yy} + \Sigma)^{-1}(y - \bar{y}), \quad (1)$$

and the error of the solution to the inverse problem can be estimated from the equation

$$\tilde{D} = K_{xx} - K_{xy}(K_{yy} + \Sigma)^{-1}K_{yx}. \quad (2)$$

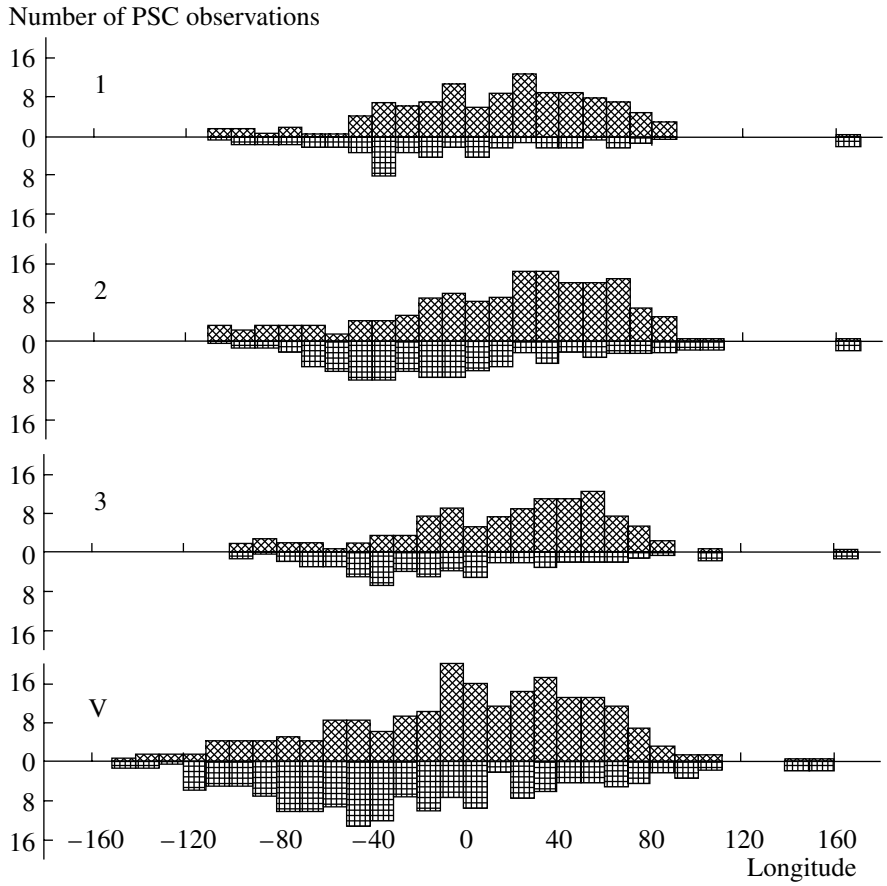

Fig. 1. Longitudinal distribution of the number of events of PSC observations in a ten-degree longitude interval according to different criteria of PSC identification (The number of observations is shown.) The upper parts of the diagrams above the abscissa axes (diagonal shading) correspond to the Northern Hemisphere, and the lower parts (straight shading) correspond to the Southern Hemisphere.

Here, x is the desired vector (in our case, four numbers: S, V, S_{NAT}, and V_{NAT}), $\bar{x}$ is its mean value; y and $\bar{y}$ are the measured vector (in our case, this is SAAC at a certain height) and its mean value, respectively; Σ is the covariance matrix of measurement errors; K is the covariance matrices of the parameters indicated in the indices; and $\tilde{D}$ is the residual uncertainty matrix (error matrix). Let us emphasize that, since the sampling according to which the solution operator is constructed is different for different criteria of PSC selection, the solution operators also differ. Therefore, for different selection criteria, different solutions (values of microphysical parameters) correspond to the same measurement. Note also that the values of errors in the SAAC measurements, which determine the components of the matrix Σ, are individual for each measured SAAC and are taken from the SAGE III data of level 2. Their values vary from 3% to values significantly exceeding the measured quantity. We considered only the measurements in which this error was less than 100%. The diagonal elements of the matrix $\tilde{D}$ made it possible to estimate the lower boundary of the errors of retrieved parameters, whose typical values were about 0.4 $\mu m^2/cm^3$ for S and S_{NAT} and 1.2 and 2.8 $\mu m^3/cm^3$ for V and V_{NAT} 1.2, respectively.

The above method allows estimation of the total microphysical parameters of an aerosol-cloud medium and the PSC component—NAT particles.

The time dependences of integral areas are in Fig. 3 for all cloud-aerosol particles, and in Fig. 4, for NAT particles. We do not give the corresponding data on integral volumes, because they demonstrate very close space and time dependences. The mean values and standard deviations of the volumes V are given in Table 5.

It follows from Figs. 3 and 4 that, in the Northern Hemisphere, there is a strong interannual variability of the total areas S and the areas of NAT particlesS_{NAT}, so that a two-year periodicity can be assumed, although this assumption is not statistically supported because of the bounded time series of observations. This variability correlates strongly with low temperatures in the stratosphere. For example, in the winter of 2004–2005, in the region of the SAGE III measure-

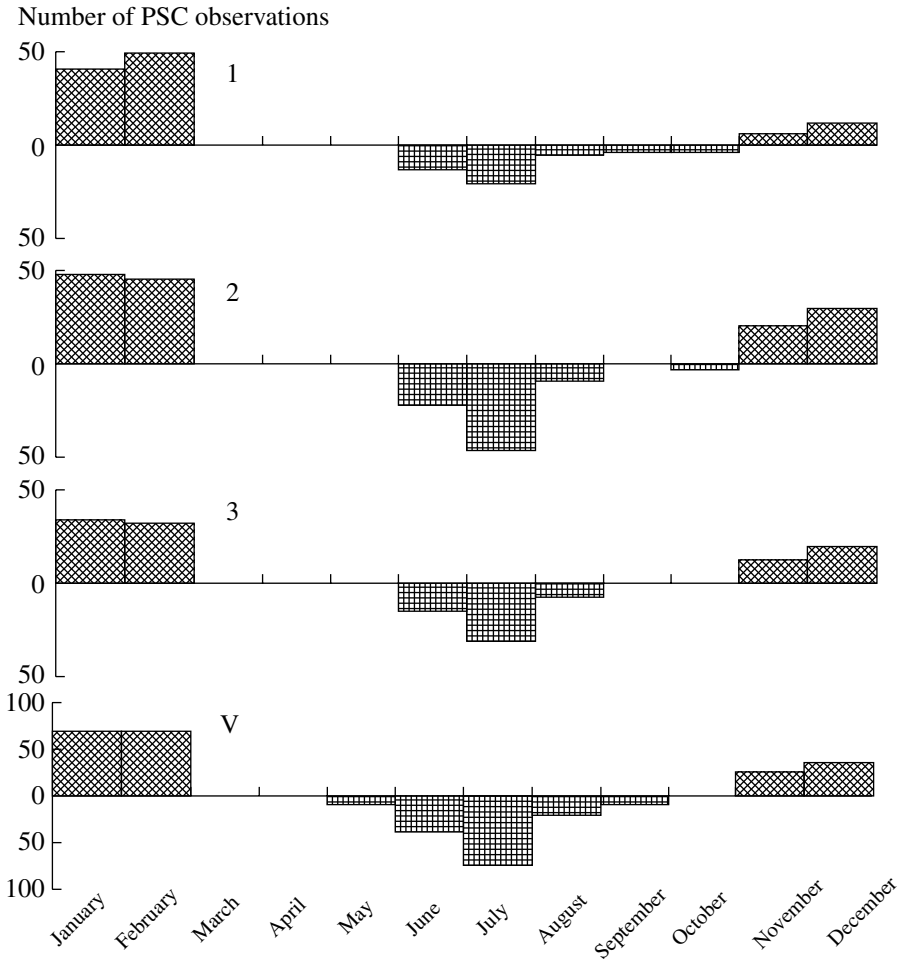

Fig. 2. Seasonal distribution of the number of events of PSC observations during a month period according to different criteria of PSC identification. The parts of the diagrams above the abscissa axes (diagonal shading) correspond to the Northern Hemisphere, and the lower parts (straight shading) correspond to the Southern Hemisphere.

ments, low temperatures were observed from early December to late February [30], which appeared to cause a large amount of PSCs and high values of their integral characteristics (see Figs. 3, 4). A small number and low values of the areas and volumes of PSC particles in the winter of 2003–2004 can, in contrast, be explained by relatively high values of stratospheric temperature.

Figures 3 and 4, as well as Fig. 2, can be used to analyze the time variability of the number of PSC occurrences, because all these graphs show the values of S and S_{NAT} only for the time of PSC observation according to the corresponding criteria. Late November–December is the usual period of PSC observation. Sometimes, PSCs are also observed in late February. For all particles (and sometimes for NAT particles), the period of PSC observation is not only November–December but also late February–early March.

The winter of 2004–2005 is distinguished by the duration of PSC observation (early November–early March) and by high values of particle areas (for PSC particles and for all particles). Thus, the total area amounts to 12–16 $\mu m^2/cm^3$. The values of S are significantly larger than those of S_{NAT}, a result that suggests that particles whose composition differs from the crystalline hydrates of nitric acid also enter the composition of observed PSCs. The relative portion of NAT particles in the total areas is mainly within 20–60%. The integral characteristics of aerosols and PSCs have high values for November–December 2002 and low values for the winter of 2003. All these results suggest a substantial interannual variability in PSCs, which is caused primarily by variations in stratospheric temperature.

The pattern of PSC observations in the Antarctic is more uniform over the years. (This is probably caused by the conditions of observations in the Southern Hemisphere—limitations in time and latitude, see Table 4.) The periods of PSC observations in the southern latitudes are as follows: early June–early October 2002, May–October 2003, and early May–

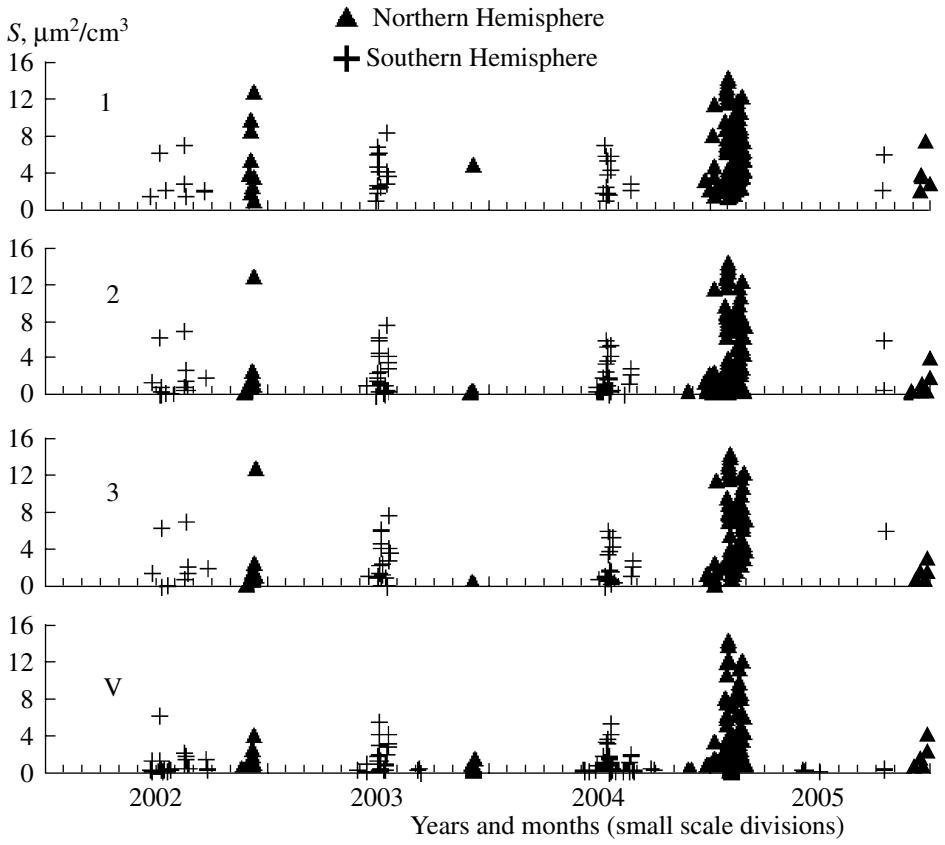

Fig. 3. Total area of all particles S according to different criteria of PSC identification

October 2004. For 2005, this period is very short: late May–early July.

Table 5 gives some statistical characteristics of the physical and microphysical parameters of cloud-aerosol particles and NAT particles for the PSCs selected according to different criteria. In Table 5, the columns present (from left to right) selection criteria in arbitrary notations (see Table 1); the height of the upper boundary of a cloud (PSC) (it should be remembered that the indicated height corresponds to a midlayer 0.5 km thick within which PSCs are observed); the height of the lower boundary of clouds; the cloud-layer thickness; the height of the layers within which PSCs are observed; the air temperature in PSCs; the area of the total surface of all particles S (the area of all fractions of PSC and the background aerosol); the total volume of the same particles V; the total surface

Table 5. Characteristics of PSCs identified with the use of different criteria

Selection method	Upper boundary, km	Lower boundary, km	Thickness, km	Mean height, km	T, K	S, $\mu m^2/cm^3$	V, $\mu m^3/cm^3$	S_{NAT}, $\mu m^2/cm^3$	V_{NAT}, $\mu m^3/cm^3$
1	21.2	18.1	3.3	19.4	191.1	4.39	4.24	0.35	1.14
	2.5	3.0	2.2	2.8	2.35	2.52	3.38	0.81	1.83
2	22.6	19.7	2.7	21.0	192.0	2.35	2.20	0.38	1.0
	2.7	3.1	2.0	2.9	2.2	2.71	3.59	0.66	1.55
3	22.0	19.8	2.1	20.9	191.6	3.01	3.03	0.45	1.18
	3.1	3.2	1.6	3.0	2.2	3.07	4.20	0.82	1.90
V_3	21.8	20.5	1.3	20.6	192.4	1.83	1.78	0.41	1.13
	2.2	2.7	1.3	2.6	2.2	2.16	3.14	0.57	1.31

Note: In each square, mean values (at the top) and standard deviations (at the bottom) are given for the entire 2002–2005 dataset.

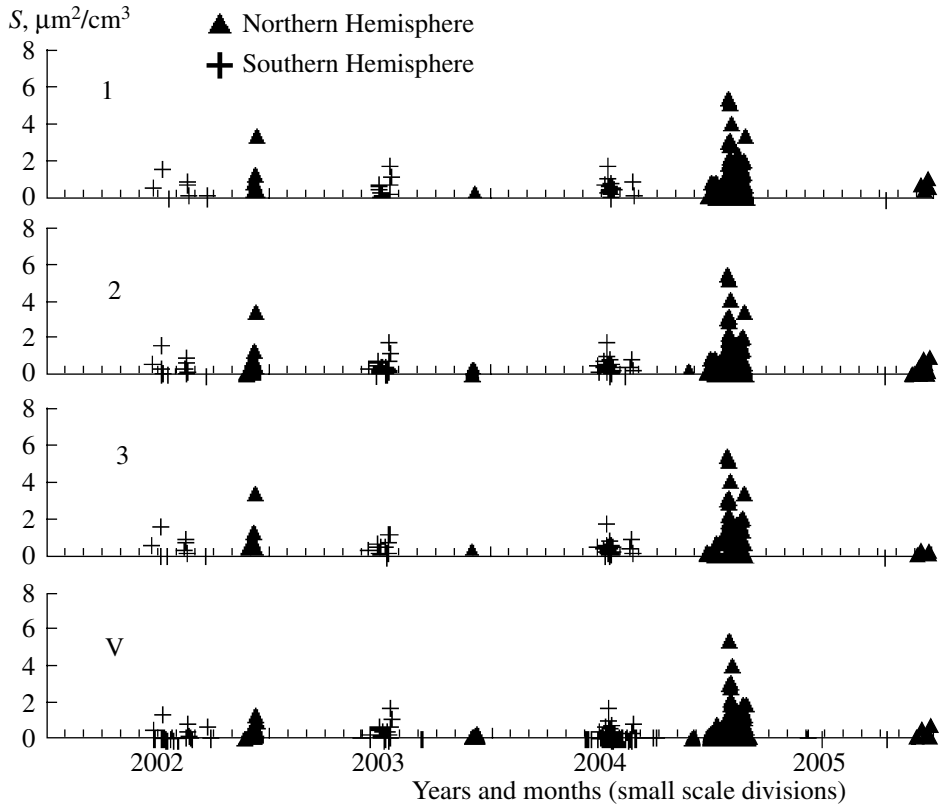

Fig. 4. Total area of NAT particles S_{NAT} according to different criteria of PSC identification.

of NAT particles S_{NAT}; and the total volume of the same particles V_{NAT}. The air temperature and integral microphysical characteristics are averaged over all PSC observations, including all heights of PSC occurrence.

In spite of the fact that certain characteristics of PSCs (for example, heights) vary only slightly with the use of different criteria of PSC selection, their microphysical characteristics can vary by a factor of 1.5–2. The value of the variability of these parameters is, to some extent, the estimate of the total error of the microphysical characteristics obtained for PSCs. Total errors are considered to mean the errors that occur owing to the influence of all factors affecting the values of the integral parameters of stratospheric aerosol: the error in measuring SAACs, the effect of the PSC-selection criterion, the adequacy of a priori information, etc.

Analysis of Table 5 shows that, for all PSC-selection criteria used in this study, the PSC parameters (both physical and microphysical) prove to be satisfactorily close to one another. Thus, for the three selection criteria, the upper boundary of the clouds deviates from the mean value by less than 0.4 km, their lower boundary deviates by 1.2 km, the air temperature deviates by 0.7 K, and S_{NAT} and V_{NAT} (the parameters of specific cloud particles) deviate by less than 20%. Thus, with sufficient confidence, these data can be treated as the estimate of the PSC parameters and the scatter of the given data describes, to a certain extent, the errors of the characteristics of interest.

3.5. Comparison with the Results of Other Studies

There are many publications on PSC observations with the use of different methods and in different years. For example, the results of the SAM II observations (1978–1979) are analyzed in [13]. The occurrence of PSCs is observed from mid-May to early November in the Antarctic and from late November to early March in the Arctic, a result that is in good agreement with our data (see Figs. 2, 4), taking into account that the SAGE III instrument takes measurements within a limited latitudinal belt and within limited time periods (Section 3.1). Namely, according to our data, the maximum probability of the occurrence of PSCs is seen from late January to early February for the Northern Hemisphere and in July for the Southern Hemisphere. The most probable longitudes of PSC occurrence (±90° from the Greenwich meridian in both hemispheres), which are indicated in this study,

are also in good agreement with our results (see Fig. 1). In [16], the results of the POAM II measurements in the Arctic during the winters of 1993–1996 are analyzed and the localization of PSCs near the Greenwich meridian in November–April is noted. This result is consistent with our observations.

In [14], on the basis of the POAM II observations in the Antarctic during 1994–1997, a broad maximum is noted at 315° of longitude (corresponds to 45* W), which is in agreement with our results for the Southern Hemisphere (see Fig. 1). According to the data presented in the same paper, the mean height of PSCs in May is 24 km, which exceeds our data by 3–4 km.

The results of direct balloon measurements of certain PSC characteristics are described in [11]. Here, variations in the physical and microphysical properties of PSCs with height are noted, which agrees with different cloud parameters (heights, microphysical parameters, etc.; see Table 5) obtained by us with the use of different selection criteria (it is quite evident that different criteria identify different types of cloud particles). The chemical, microphysical, and optical characteristics of PSCs are also given in [11]. The volume of all particles from the measurements taken on January 25, 2000, which is given in graph form, is of interest to us. This quantity varies in clouds from tenths to 10 $\mu m^3/cm^3$, which does not contradict the data given in Table 4 (the maximum means are 1.8–4.1 $\mu m^3/cm^3$ for the layer 500 m thick). According to the POAM III data obtained in 1999–2000 in the Arctic, PSC heights of 18 to 23 km and the maximum frequency of PSC occurrence in January have been noted in [5].

The evolutions of the polar vortex and PSCs during the winter of 2002–2003 are analyzed on the basis of MIPAS data in [17]. Analysis of the PSC composition has shown the presence of NAT particles in December, but a small number of them after December. This conclusion is in good agreement with our results given in Fig. 4, which shows that, unlike the winter of 2004–2005, in 2002–2003, according to the SAGE III data, almost all PSCs were observed in early December.

The PSC climatology from lidar measurements taken in the Spitsbergen region in 1994–2004 is given in [31]. During this period, there were five winters when the stratospheric temperatures over Scandinavia were low enough to form PSCs. The typical heights of cloud occurrence, 20–24 km, actually coincide with our data.

Thus, it is possible to conclude that, in general, the PSC parameters obtained from the SAGE III observations agree well with the data obtained from earlier independent measurements.

4. BASIC RESULTS AND CONCLUSIONS

(1) The PSC identification criteria using the results of SAAC measurements are considered and verified on the basis of model and real data. A new criterion based on a statistical simulation of PSC and the BSA is proposed. It is shown that the use of different criteria can result in differences in the selected ensembles of PSCs, which, of course, can, to a certain extent, affect the climatological characteristics of PSCs. In these methods, it makes sense to use not only the results of SAAC measurements but also additional data, in particular, on stratospheric temperature.

(2) Seasonal, interannual, and longitudinal variations in the frequency of PSC occurrence in the polar regions of both hemispheres are analyzed on the basis of the SAGE III measurements from March 2002 to December 2005. It is shown that, in accordance with the earlier measurements, PSCs are most likely to occur in winter: December–February for the Northern Hemisphere and June–August for the Southern Hemisphere. Significant interannual variations in the frequency of occurrence of PSCs and their integral microphysical characteristics are observed. In particular, in the winter of 2004–2005, a large amount of PSCs and high values of the total areas and volumes of PSCs were noted. The longitudes of the most probable occurrence of PSCs are determined. In the Northern Hemisphere, PSCs are observed in the longitudinal sector 120°W–100°E, with the maximum frequency of their occurrence near the Greenwich meridian. A large portion of PSCs r observed in the sector ±80° near the zero meridian. In the Southern Hemisphere, the region of PSC occurrence is almost the same in longitude, but with these are westward shift of the region characterized by the maximum frequency of PSC occurrence. The maximum occurrence is observed near 40° W, and the usual region of occurrence is 40°W ± 60°.

(3) The mean values and variations of the height of PSCs are determined for the Northern and Southern hemispheres. For the regions and periods of measurements with the SAGE III instrument, the mean heights of the lower and upper boundaries of PSCs are 19.5 ± 1 and 21.9 ± 0.6 km, respectively, at a standard deviation of 3.0 and 2.6 km. The mean temperature in clouds is 191.8 ± 0.5 K at a standard deviation of 2.2 K. The mean cloud thickness is 2.4 ± 0.9 km at a standard deviation of 1.8 km.

(4) The inverse problem of determining the integral microphysical characteristics of PSCs—the total areas and volumes of all aerosol-cloud particles and NAT particles—is solved with the use of the linear regression method. The mean integral microphysical parameters of PSCs over the entire observation period (2002–2005) have the following values: the total area of NAT particles $S_{NAT} = 0.41 \pm 0.04$ $\mu m^2/cm^3$ at a standard deviation of 0.8 $\mu m^2/cm^3$ and the total volume of

NAT particles $V_{NAT} = 1.1 \pm 0.1$ $\mu m^3/cm^3$ at the standard deviation less than 1.8 $\mu m^2/cm^3$. For all cloud and aerosol particles in the PSC volume, $S = 2.9 \pm 1.5$ $\mu m^2/cm^3$ at a standard deviation of 2.7 $\mu m^2/cm^3$ and $V = 2.8 \pm 1.5$ $\mu m^3/cm^3$ at a standard deviation of 4.2 $\mu m^3/cm^3$.

(5) The data are compared to the results of earlier lidar, balloon (direct), and satellite measurements of PSC characteristics. A good agreement with all data on the spatiotemporal location of aerosol-cloud formations and on their physical and integral microphysical parameters is obtained.

ACKNOWLEDGMENTS

The SAGE III data were provided by the NASA Langley Research Center Atmospheric Sciences Data Center.

This study was supported by the Russian Foundation for Basic Research (project nos. 05-05-65305-a and 06-05-64909-a) and the Ministry of Education and Science (grant nos. RNP.2.1.1.4166 and RNP.2.2.1.1.3836).

REFERENCES

1. S. Solomon and R. R. Garcia, et al., "On the Depletion of Antarctic Ozone," Nature **321**, 755–758 (1986).
2. *World Meteorological Organization (WMO), Scientific Assessment of Ozone Depletion: 1994,* WMO Report 37 (WMO, Geneva, 1995).
3. L. C. Sloan and D. Pollard, "Polar Stratospheric Clouds: A High Latitude Warming Mechanism in an Ancient Greenhouse World," Geophys. Rev. Lett. **25**, 3517–3520 (1998).
4. J. H. Seinfeld and S. N. Pandis, *Atmospheric Chemistry and Physics. From Air Pollution to Climate Change* (Wiley, New York, 1998).
5. A. W. Strawa, K. Drdla, M. Fromm, "Discriminating Types Ia and Ib Polar Stratospheric Clouds in POAM Satellite Data," J. Geophys. Res. D **107**, doi: 10.1029/2001JD000458, 8291 (2002).
6. K. Drdla, *Applications of a Model of Polar Stratospheric Clouds and Heterogeneous Chemistry* (PhD Thesis, UCLA, 1996).
7. K. Drdla, M. R. Shoeberl, and E. V. Browell, "Microphysical Modeling of the 1999–2000 Arctic Winter," J. Geophys. Res. D **108**, 8312 (2003).
8. Ya. A. Virolainen, Yu. M. Timofeev, A. V. Polyakov, et al., "Modeling Polar Stratospheric Clouds: I. Microphysical Characteristics," Opt. Atmos. Okeana **18**, 264–269 (2005).
9. Ya. A. Virolainen, Yu. M. Timofeev, A. V. Polyakov, et al., "Modeling Polar Stratospheric Clouds: II. Statistics of the Spectral Attenuation Coefficient and Possibilities of PSC Remote Sensing," Opt. Atmos. Okeana **18**, 586–591 (2005).
10. M. P. McCormic, H. Steele, et al., "Polar Stratospheric Cloud Sighting by SAM II," J. Atmos. Sci. *39*, 1387–1397 (1982).
11. J. Schreiner, C. Voigt, et al., "Chemical, Microphysical and Optical Properties of Polar Stratospheric Clouds," J. Geophys. Res. D *108*, doi: 10.1029/2001JD000825, 8313 (2003).
12. M. P. McCormick and C. R. Trepte, et al., "Persistence of Polar Stratospheric Clouds in Southern Polar Region," J. Geophys. Res. D *94*, 11 241–11 251 (1989).
13. L. R. Poole and M. C. Pitts, "Polar Stratospheric Cloud Climatology Based on Stratospheric Aerosol Measurement II Observations from 1978 to 1989," J. Geophys. Res. D *99*, 13 083–13 089 (1994).
14. M. D. Fromm, J. D. Lumpe, et al., "Observation of Antarctic Polar Stratospheric Clouds by POAM II: 1994–1996," J. Geophys. Res. D *102*, 23 659–23 672 (1997).
15. Y. Kim, W. Choi, K.-M. Lee, et al., "Polar Stratospheric Clouds Observed by the ILAS-II in the Antarctic Region: Dual Compositions and Variation of Compositions during June to August of 2003," J. Geophys. Res. *111*, doi: 10.1029/2005JD006445, D13S90 (2005).
16. S. T. Massie, D. Baumgardner, and J. E. Dye, "Estimation of Polar Stratospheric Cloud Volume and Area Densities from UARS, Stratospheric Aerosol Measurement II, and Polar Ozone and Aerosol Measurement II Extinction Data," J. Geophys. Res. D *103*, 5773–5784 (1998).
17. R. Spang, J. J. Remedios, L. J. Kramer, et al., "Polar Stratospheric Cloud Observations by MIPAS on ENVISAT: Detection Method, Validation and Analysis of the Northern Hemisphere Winter 2002/2003," Atmos. Chem. Phys. *5*, 679–692 (2005).
18. A. V. Polyakov, YuM. Timofeyev, D. V. Ionov, et al., "Newchurch Retrieval of Ozone and Nitrogen Dioxide Concentration from Stratospheric Aerosol and Gas Experiment III (SAGE III) Measurement Using a New Algorithm," J. Geophys. Res. *110*, doi: 10.1029/2004JD005060, D06303 (2005).
19. A. V. Polyakov, Yu. M. Timofeev, D. V. Ionov, et al., "New Interpretation of Transmittance Measurements by the SAGE-III Satellite Spectrometer," Izv. Akad. Nauk, Fiz. Atmos. Okeana *41*, 410–422 (2005) [Izv., Atmos. Ocean. Phys. *41*, 371–382 (2005)].
20. A. M. Chaika, Yu. M. Timofeev, and A. V. Polyakov, "Stratospheric Aerosol from the Data of SAGE III Measurements," Issled. Zemli Kosmosa, No. 2, 10–18 (2007).
21. G. S. Eent and M. P. McCormick, "Separation of Cloud and Aerosol in Two-Wavelength Satellite Occultation Data," Geophys. Res. Lett. *18*, 428–431 (1991).
22. M. C. Pitts, L. R. Poole, and M. P. McCormick, "Climatology of Polar Stratospheric Clouds Determined from SAM II Observations," in *Digest of Topical Meeting on Optical Remote Sensing of the Atmosphere* (Optical Society of America, Washington, 1990), Vol. 4, pp. 206–209.
23. G. K. Yue and M. P. ChuW. McCormic, "P. Retrieval of Composition and Size Distribution of Stratospheric Aerosol with the SAGE II Satellite Experiment," J. Atmos. Ocean. Technol. *3*, 371–380 (1986).

24. M. H. Hitchman, M. McKay, and C. R. Trepte, "A Climatology of Stratospheric Aerosol," J. Geophys. Res. D *99*, 20 689–20 700 (1994).
25. G. S. Kent, P.-H. Wang, and R. M. Skeens, "Discrimination of Cloud and Aerosol in the Stratospheric Aerosol and Gas Experiment III Occultation Data," Appl. Opt. *36*, 8639–8649 (1997).
26. G. S. Eent, C. R. Trepte, et al., "Problems in Separating Aerosol and Clouds in the Stratospheric Aerosol and Gas Experiment (SAGE) II Data Set under Conditions of Lofted Dust: Application to the Asian Deserts," J. Geophys. Res. D *108*, doi:10.1029/2002JD002412, 4410 (2003).
27. Ya. A. Virolainen, Yu. M. Timofeev, A. V. Polyakov, et al., " Analysis of Solutions to the Inverse Problem on the Retrieval of the Microstructure of Stratospheric Aerosol from Satellite Measurements," Izv. Akad. Nauk, Fiz. Atmos. Okeana *42*, 816–829 (2006) [Izv., Atmos. Ocean. Phys. *42*, 752–764 (2006)].
28. *Airborne Arctic Stratospheric Expedition*, (CD-ROM), ed. by S. Hipskind and S. Gaines (NASA Ames Research Center, 1995).
29. *Airborne Southern Hemisphere Ozone Experiment and Measurements for Assessing the Effects of Stratospheric Aircraft* (CD-ROM), ed. by S. Gaines (NASA Ames Research Center, 1995).
30. www.cpc.ncep.gov/products/stratosphere
31. P. Massoli, M. Maturilli, and R. Neuber, "Climatology of Arctic Polar Stratospheric Clouds As Measured by Lidar in Ny-Alesund, Spitsbergen (79° N, 12° E)," J. Geophys. Res. **111**, doi:10.1029/2005JD005840, D09206 (2006).

SPELL: 1. Pandis